BIOCHEMISTRY
including biophysical chemistry & molecular biology

Article

pubs.acs.org/biochemistry

Role of Peptide–Peptide Interactions in Aggregation: Protonectins Observed in Equilibrium and Replica Exchange Molecular Dynamics Simulations

Gisele Baldissera,[†,§] Marcia Perez dos Santos Cabrera,*[,‡,†] Jorge Chahine,[†] and José Roberto Ruggiero[†]

[†]Departamento de Física, [‡]Departamento de Química e Ciências Ambientais, Universidade Estadual Paulista, 15054-000 São José do Rio Preto, SP, Brazil

[§]Faculdade de Tecnologia de Catanduva, 15800-020 Catanduva, SP, Brazil

Supporting Information

ABSTRACT: Protonectin (ILGTILGLLKGL-NH_2), a peptide extracted from the venom of the wasp *Agelaia pallipes pallipes*, promotes mast cell degranulation activity, antibiosis against Gram-positive and -negative bacteria, and chemotaxis in polymorphonucleated leukocytes. Another peptide from the same venom, Protonectin (1−6), corresponding to the first six residues of Protonectin, exhibits only chemotaxis. A 1:1 mixture of these two peptides showed positive synergistic antimicrobial effects, attributed to the formation of a heterodimer.[16] The antimicrobial activity is probably related to the peptides' interaction with membrane phospholipids. Equilibrium and replica exchange molecular dynamics simulations were used to investigate two systems: the interaction of Protonectins (two molecules) and that of a mixture Protonectin and Protonectin (1−6) in the environment of sodium dodecyl sulfate (SDS) micelles, which mimic bacterial membranes and are also highly anionic. We found that in both systems the peptides tend to aggregate in the aqueous environment and are held together by hydrophobic interactions and hydrogen bonds. In the equilibrium simulations, aggregated Protonectin/Protonectin (1−6) dissociates after penetrating the SDS micelle, whereas the two Protonectins remain associated throughout the simulation time. Also, in the replica exchange simulations, the Protonectins remain closer, associating through a greater number of hydrogen bonds, and were found at only one free energy minimum, whereas the peptides in the mixture display other probable distances from each other, which are significantly longer than those observed with two Protonectin molecules. Coulomb contributions and the free energy of the systems containing micelles were calculated and show that the interactions of the mixed peptides are favored, whereas the interactions between pure Protonectins are more probable. As a consequence of the preferential interaction with the micelle, the Protonectin molecule of the mixed system presents a higher helical structure content. The enhancement of the amphipathic features caused by Protonectin (1−6) can be related to the increase in the antimicrobial activity experimentally observed.

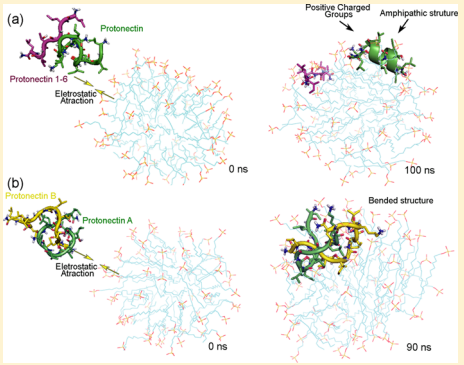

Antimicrobial peptides (AMPs) constitute an important component of wasp venoms because of their abundance and diversity.[1−3] The efficacy and broad spectrum of biological activities of some short chain length AMPs make them attractive molecules to synthesize in the search for new antibiotics.[4−6] However, knowledge of the biological significance of the many homologous sequences present in a single species is limited. In some cases, investigations have demonstrated that related peptides show synergism in their activities.[7,8]

Synergistic effects between AMPs are an interesting area of investigation because of the possibility of lowering the concentration of active peptides, broadening their effectiveness, and reducing their toxicity.[8] A hallmark of these studies is the association of magainin and PGLa to form heterodimers or heterosupramolecular complexes that have been investigated by fluorescence and NMR methods.[9−11] Other examples involve synergy between dermaseptins[12] or temporins[13] and antimicrobial and anticancer peptides used as current treatments.[6,8]

Recently, a pair of peptides was extracted from the venom of the social wasp *Agelaia pallipes pallipes* and identified as Protonectin (ILGTILGLLKGL-NH_2) and Protonectin 1−6 (ILGTIL-NH_2).[14] Protonectin (PTN) is an antimicrobial peptide that was originally found in the venom of the social wasp *Protonectarina sylveirae*.[15] Its biological activity and structural properties were investigated in a 1:1 molar mixture with Protonectin (1−6), (PTN_{1-6}), by Baptista-Saidemberg et al.[16] These authors verified that this mixture presents positive synergistic effects with regard to biological activities, which are dependent on membrane interactions. They found a modest increase in the hemolytic and mast cell degranulation activities of the PTN/PTN_{1-6} mixture relative to the activity of PTN, which is compatible with the increased hydrophobicity of the

Received: September 25, 2014
Revised: February 28, 2015
Published: March 17, 2015

DOI: 10.1021/bi501210e
Biochemistry 2015, 54, 2262−2269

Table 1. Summary of Simulations

simulation	peptides	environment	time (ns)	protocol
PTN	Protonectin/Protonectin	water; 8986 molecules; 4 Cl^-	150	equilibrium simulation
PTN_{1-6}	Protonectin/Protonectin 1−6	water; 4027 molecules; 3 Cl^-	150	equilibrium simulation
PTN	Protonectin/Protonectin	SDS micelle; 19 225 water molecules; 65 Na^+; 4 Cl^-	100	equilibrium simulation
PTN_{1-6}	Protonectin/Protonectin 1−6	SDS micelle; 10 325 water molecules; 65 Na^+; 3 Cl^-	100	equilibrium simulation
PTN	Protonectin/Protonectin	SDS micelle; 19 225 water molecules; 65 Na^+; 4 Cl^-	24 × 100	REMD
PTN_{1-6}	Protonectin/Protonectin 1−6	SDS micelle; 10 325 water molecules; 65 Na^+; 3 Cl^-	24 × 100	REMD

mixture (from 0.276 to 0.323) and the MIC reduction observed for Gram-positive bacteria (*Bacillus subtilis* (68%) and *Staphylococcus aureus* (34%)) and Gram-negative bacteria (*Escherichia coli* (67%) and *Pseudomonas aeruginosa* (35%)) calculated on a molar basis. PTN and PTN_{1-6} also promote the chemotaxis of mast cells toward polymorphonuclear leukocytes, but only the shorter peptide displays this chemotactic activity. Notable structural features of these peptides include the following: (1) the sequence of PTN_{1-6} corresponds to the first six amino acid residues of PTN; (2) PTN is composed of hydrophobic amino acids, with a single charged lysine residue at position 10, whereas PTN_{1-6} has only hydrophobic amino acids; (3) both have an amidated C-terminus, which contributes +1 to the net charge. PTN can associate with PTN_{1-6} to form a more hydrophobic complex, and the presence of a heterodimer has been hypothesized based on MS-ESI data.[16]

In the present work, we investigated peptide−peptide interactions to search for possible aggregation between PTNs and PTN/PTN_{1-6}, to determine how it could occur, and to characterize the influence of the environment on the aggregation. To this end, theoretical computational model systems, using SDS micelles, were subjected to equilibrium MD simulations complemented by replica exchange MD (REMD). This theoretical method avoids bias due to initial configurations and is more efficient for scanning conformational space,[17−19] improving the accuracy of calculating the free energy of the systems. Through this calculation, we showed that aggregation is possible for PTNs and for PTN/PTN_{1-6}; however, the latter pair has a lower probability to form.

EXPERIMENTAL PROCEDURES

Models and Methods. Molecular dynamics (MD) simulations have been increasingly used to elucidate experimental data.[20−23] Although simulations using lipid bilayers may demonstrate a comprehensive picture of peptide−membrane interaction, simpler membrane mimetic environments, such as TFE/water mixtures and micelles, also reveal important details of these interactions at lower computational costs.[24−29] Additionally, many recent studies of antimicrobial peptides have demosntrated correlations between molecular dynamics simulations in micelles, either zwitterionic or anionic, and structural data obtained from NMR experiments in these same model membranes.[30] SDS micelles provide some of the essential features provided by lipid bilayers that are involved in their interaction with peptides, such as a hydrophobic alkyl/acyl chain region, a hydrophilic shell formed by the headgroup region, and an interfacial environment between the surfaces and the aqueous environment. Nevertheless, a higher intrinsic curvature radius, the presence of lone alkyl chains, and the ease of deformation are limitations of this model that must be taken into account.[24,27]

Molecular Dynamics (MD) Simulations. Simulations were performed in cubic boxes of various sizes to accommodate the different systems and with enough water molecules to guarantee the water density. Ideal α-helical configurations were generated by RIBOSOME V1.0 software.[31] Two PTN molecules (or one PTN and one PTN_{1-6}) in these configurations, separated by approximately 2 nm, were placed in a box with water molecules (and enough Cl^- ions for neutralization) and simulated for 150 ns. These simulations in water were used to obtain random conformations of the peptides. The components of the studied systems are a preformed SDS micelle, consisting of 65 SDS molecules, water molecules, enough counterions for neutralization, and two peptide molecules from the simulations in water. In this study, we use an SDS micelle obtained by T.R. Valder.[32] The configurational parameters of this model micelle are in good agreement with the literature with respect to the number of SDS monomers,[33,34] eccentricity, radius, and area.[35−38]

Two independent equilibrium simulations were run in this system for 100 ns, one for each peptide pair, and compared with another two simulations using the replica exchange method. In these simulations, the two peptide molecules were placed in the aqueous environment. Their centers of mass were placed around 3.0 nm from the center of the micelle. The average radius of the micelle was 1.9 nm (average distance between the sulfur atoms and the center of mass of the micelle); the eccentricity of the micelle was determined in the absence of peptides, and it was maintained in their presence. Table 1 summarizes the set of simulations performed in the present work.

Conditions and Evaluation. Simulations were performed and analyzed using the Gromacs 4.0.7 package,[39,40] with the NPT ensemble. GROMOS force field[41] sets were used on the basis of the system to be simulated: 43A1 (simulations in water)[42] and 45A3 (simulations in SDS).[43−45] The main difference between force fields 43A1 and 45A3 is related to the parameters for long aliphatic chains (CH_2 > 6 units) that influence SDS aliphatic chains.[26,43,44] The long-range electrostatic interactions were treated by the particle mesh Ewald (PME) method,[46,47] using a cutoff radius for the Coulomb and the Lennard-Jones interactions of 1.0 nm. The neighbor list was updated every 10 time steps. All bonds were constrained using the LINCS algorithm[48] and the SETTLE algorithm.[49] The SPC model was used for water molecules.[50] System optimization for the equilibrium simulations was carried out with the steepest descent method considering convergence criteria of 10^{-2} kJ mol^{-1} or in 300 000 steps of integration. Position restriction dynamics for solvent and ions relaxation ran for 2 ns. The time step for integrating the equations of motion was 2 fs, and the data were recorded every 10 ps.

Simulations using the REMD were performed with 24 temperature values in the range from 288 to 315.6 K, with a rate of exchange of 3000 steps. The exchange rate showed an

DOI: 10.1021/bi501210e
Biochemistry 2015, 54, 2262−2269

acceptance of approximately 40% among replicas. Analyses were performed considering data from the last 50 ns of simulation time. A free energy surface map was generated with the WHAM algorithm.[51,52]

RESULTS AND DISCUSSION

It has been demonstrated that a mixture of PTN and PTN_{1-6} at a 1:1 molar ratio potentiates the biological activities of these peptides with regard to membrane perturbation in comparison to the activity of Protonectin.[16] The same study also showed that PTN exhibits spectra indicative of helical structure in the presence of a trifluoroethanol/water mixture or in the presence of a micellar SDS solution. Although the helical content is low, it is increased by the presence of PTN_{1-6} at a 1:1 molar ratio. To verify that Protonectin can interact with anionic lipid vesicles made of phosphatidylcholine (PC) mixtures with phosphatidylglycerol (PG, 30 and 60%) and with cardiolipin (CL, 30%), which are also used as bacterial membrane mimetic environments, CD spectra were acquired. In buffer, spectra are characteristic of unordered structures, and the presence of anionic vesicles induces a significant conformational change, as demonstrated by the negative bands at 207−208 and 222 nm that are characteristic of helical structures (Supporting Information, Figure S1). These findings show that SDS micelles and phospholipid bilayers induce a similar structure in PTN, which may target the phospholipid matrix of bacterial membranes, although other targets cannot be excluded.

Searching for Peptide Aggregation: Simulations in Water. Mass spectra acquired in an aqueous environment for a 1:1 mixture of PTN and PTN_{1-6} showed peaks corresponding to a heterodimer.[16] However, simulations in water demonstrated that the homodimer, PTN/PTN, is more probable than the heterodimer, PTN/PTN_{1-6}, although both occur (Figure 1). The secondary structure profiles for PTNs and PTN/PTN_{1-6} (Supporting Information, Figure S2) indicate that the starting α-helical configuration is quickly lost (in some cases, during the energy-minimization step) and that the peptides assume predominantly random conformations. The trajectory analysis shows that the contact between the peptides starts within approximately 15 ns and remains throughout the simulation (Figure 1a). Also, the peptides associate through hydrogen bonds that are greater in number in the simulation of the PTNs (on average, 5.5; Figure 1b) than that in the PTN/PTN_{1-6} simulation (on average, 2.3; Figure 1c). The association of the peptides minimizes their contacts with water. This is indicated by the reduction in the hydrophobic surface areas accessible to the solvent, which are approximately 10 and 18% smaller for the PTN/PTN_{1-6} mixture and the pure PTNs, respectively, when compared to their condition before aggregation. The association process in both cases significantly reduced (about 50%) the number of water molecules in the first layer of hydration (approximately 4 Å). These results suggest that the association in water is caused by hydrophobic forces along with hydrogen bonds.

Investigating Peptide Aggregation and the Influence of the Environment: Simulations in SDS. The pattern of the secondary structures adopted by the peptide pairs in the equilibrium simulations indicates that the micelle environment induces the two PTN molecules to preferentially assume bended structures. In the simulations of PTN/PTN_{1-6}, the PTN molecule often assumes helical conformations, such as α- and π-helix, and the shorter PTN_{1-6} remains in a random conformation (Supporting Information, Figure S3). Analysis of

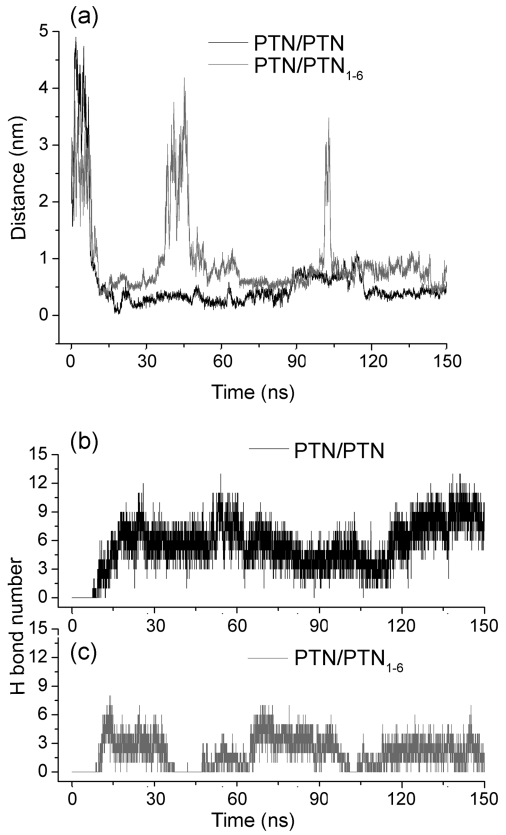

Figure 1. PTNs and PTN/PTN_{1-6} interactions in water. (a) Distance between PTNs (black) or PTN and PTN_{1-6} molecules (gray). (b) Hydrogen bonds between PTNs. (c) Hydrogen bonds between PTN and PTN_{1-6} molecules.

these trajectories shows that insertion into the SDS micelle is rapid (Figure 2a), approximately 3 ns for PTN/PTN_{1-6} and 10 ns for PTNs. After insertion, the center of mass of the peptide(s) oscillates relative to the center of the micelle, with individual time-averaged values of 1.3 ± 0.1 nm and 1.4 ± 0.3 nm for the PTNs and 1.4 ± 0.3 nm and 1.5 ± 0.3 nm for PTN/PTN_{1-6}. The radius of gyration of the micelle containing the peptides is approximately 1.66 ± 0.02 nm for PTNs and 1.64 ± 0.06 nm for PTN/PTN_{1-6}, which indicates that the peptides' centromers remain in the environment of the alkyl hydrophobic tails of the SDS molecules for most of the time. Figure 2b,c shows that after insertion in the micelle the PTNs remain close to each other due to the presence of 8.3 hydrogen bonds, on average, whereas PTN and PTN_{1-6} lose the hydrogen bonds formed in water and separate. As shown in Figure 2b, the distance between the peptides increases to something close to 3 nm, the diameter of the micelle. Solvation analysis (Figure 2d) of C_α of each residue of the two PTNs shows that both molecules are predominantly solvated by the alkyl chain tails of the SDS molecules. In the PTN/PTN_{1-6} system, PTN's residues show an abundance of charged SO_4^{2-} head groups around C_α of residues 1, 2, 5, and 6, whereas C_α of residues 3, 7, 8, and 9 is surrounded by the alkyl tails of the SDS molecules. The remaining C_α are at the interface between these two regions. These data, along with the secondary structure profile, indicate that PTN of the PTN/PTN_{1-6} system assumes a more amphipathic conformation.

Although the insertion and localization of the peptides were expected because of the anionic nature of the micelle and the

DOI: 10.1021/bi501210e
Biochemistry 2015, 54, 2262−2269

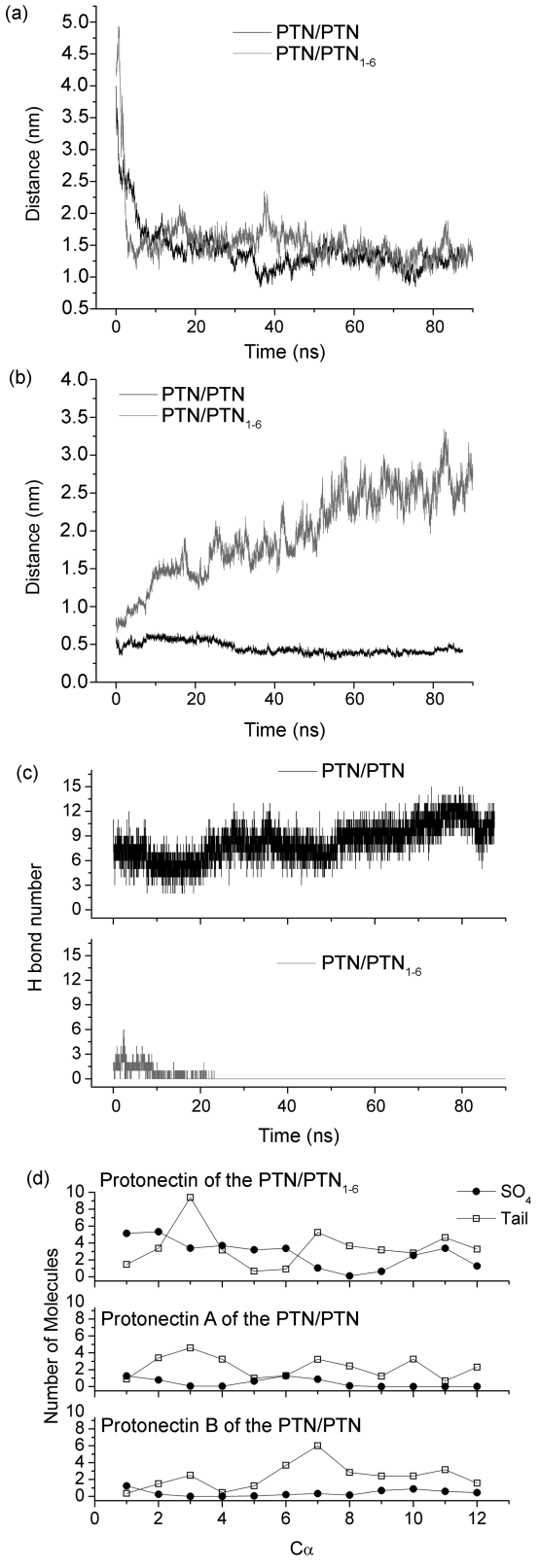

Figure 2. Characteristics of PTNs and PTN/PTN_{1-6} interactions in the presence of SDS micelles. (a) Distance between the center of mass of the peptides and the center of mass of the SDS micelle along the simulation time. (b) Distance and (c) hydrogen bonds (H bonds) between the peptide molecules. PTNs are represented in black, and PTN/PTN_{1-6} molecules, in gray. (d) Solvation profile around C_α residues. PTN in the PTN/PTN_{1-6} simulations, upper part; PTNs in the pure PTN simulations, center and lower parts.

positive charges of the peptides, it was unexpected that PTN/PTN_{1-6} would exhibit a different association pattern than that of PTNs in SDS micelles.

Comparing Equilibrium Simulations with Replica Exchange Results. To exclude the possibility that the results from the equilibrium simulations are biased by the initial configuration of the peptides, REMD was used. The potential energy histograms indicate that a larger conformational space exists in the REMD simulations (Supporting Information, Figure S4) in comparison to the potential energy distribution for the equilibrium simulations. REMD provides a broader scan of the conformational space than that with equilibrium simulations, preventing the system from being trapped in local energy minima. Trajectories from the replica exchange simulations and the WHAM package were used to obtain the free energy surface versus the number of residues in α-helical conformation and versus the distance between the peptides (Figure 3). This analysis revealed that there is a significant higher probability for the mixed peptides system to visit a larger conformational space than there is for the pure PTNs system. For PTNs (Figure 3a), only one minimum is observed, and distances longer than 1.25 nm are not visited. A representative configuration from this minimum is shown for comparison with a higher free energy configuration, in which some helical residues appear. It is also observed that the peptides are close to each other and that this is independent of the number of helical residues. With PTN/PTN_{1-6}, three free energy minima are observed, and distances as long as 3 nm were found between the peptides' centromers (Figure 3b). In the main minimum, the representative configuration is also poorly helical, as shown for PTNs, but in this case, the peptides are farther from each other. In the second minimum, the peptides remain at the same distance, but the helical content increased significantly. In the third minimum, the representative configuration shows separated peptides, and the helical conformation is maintained. The increased helical content of the PTN/PTN_{1-6} mixture in relation to that of the pure PTNs is in good agreement with experimental data and with the increased amphipathicity shown in the equilibrium simulations (Figure 2d).

The histogram of the distances between the peptides' centromers (Figure 4a) in the equilibrium simulations also shows that PTNs are found, most probably, closer to each other, as opposed to the PTN/PTN_{1-6} system, in which the peptides are often apart. To compare the structures from the equilibrium simulations with those from the REMD (Figure 3a,b), RMSDs between these structures were calculated, and a histogram of these values was plotted. Figure 4b shows the RMSD histogram obtained for the structures of the PTN/PTN_{1-6} system at the third minimum as an example. RMSD values around 0.3 nm and lower indicate that most of the structures obtained in the equilibrium simulations represent the reference structure obtained in REMD. Also, the histograms show that PTNs structures are less changeable than that of PTN in the PTN/PTN_{1-6} system.

The Tendency toward Aggregation Is Different between PTNs and PTN/PTN_{1-6} and Differently Affects the Peptides' Interaction with SDS Micelles. The peptide−peptide interaction of PTNs occurs at a shorter distance (0.5 nm) and is energetically favored in relation to that in PTN/PTN_{1-6} (Figure 5). The free energy surface versus the distance between the peptides' centromers and versus the sum of the Coulomb and Lennard-Jones contributions to the interaction energy (pairwise averaged) exhibits a minimum in

DOI: 10.1021/bi501210e
Biochemistry 2015, 54, 2262−2269

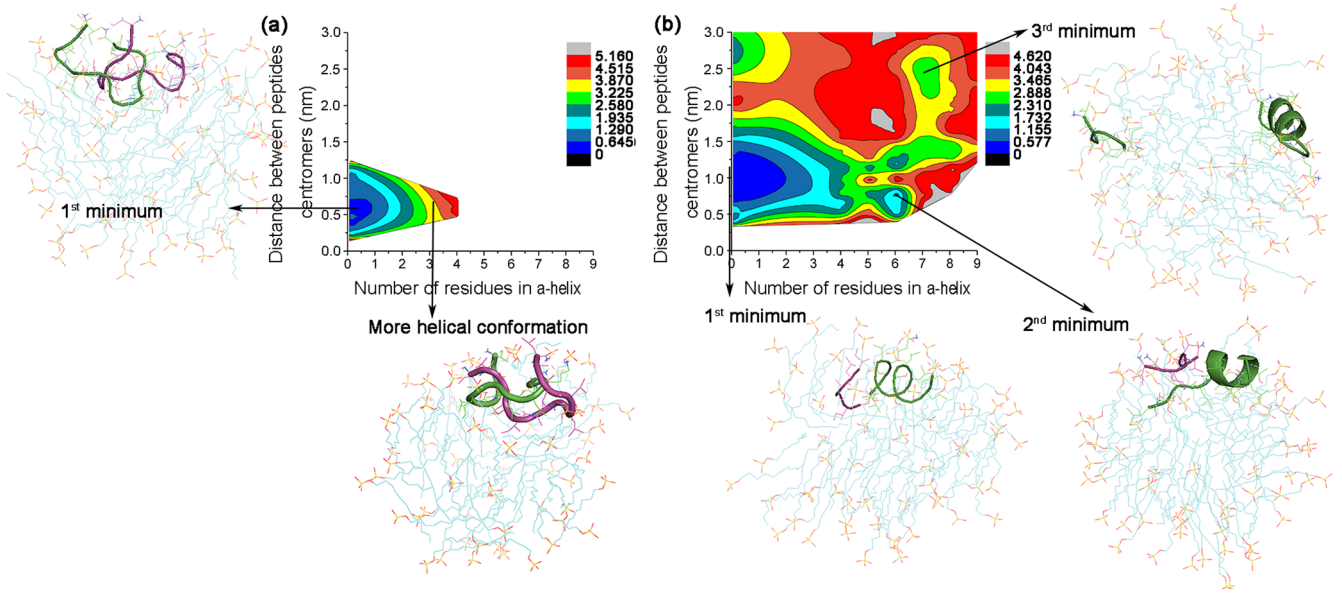

Figure 3. Free energy map (kcal mol^{-1}) versus the number of residues in α-helix conformation and versus the distance between the peptides' centromers, obtained from REMD simulations in the presence of SDS micelles, as well as the representative configurations of the principal minima: (a) PTNs and (b) PTN/PTN_{1-6}.

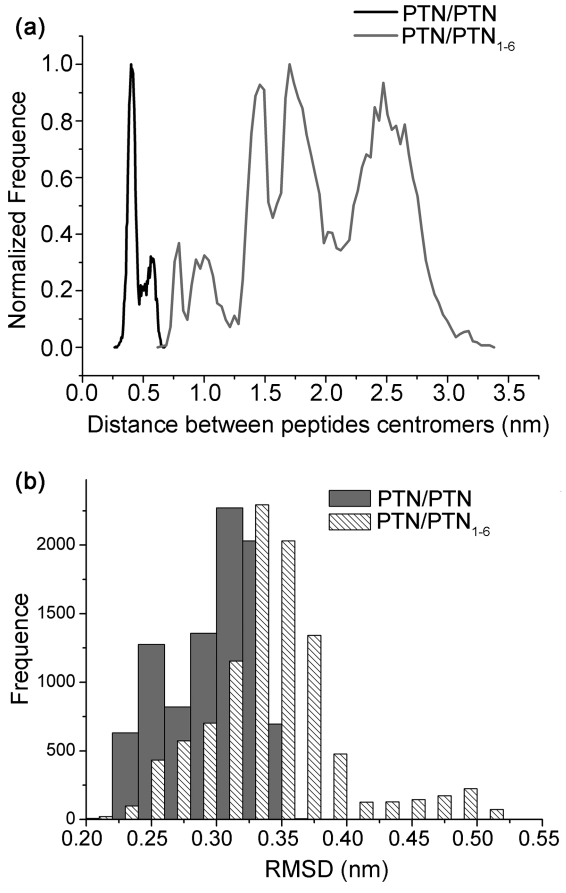

Figure 4. Comparison of results obtained from equilibrium simulations and the replica exchange method. (a) Histogram of the distance between the peptides' centromers in the equilibrium simulations. (b) Histogram of the RMSD between one of the representative conformations obtained in the REMD and the structures of each frame of the equilibrium simulations.

the PTN/PTN system in the range of -12.10^{-3} to -10.10^{-3} kcal mol^{-1}, whereas for PTN/PTN_{1-6}, the minimum is in the range of -9.10^{-3} to -6.10^{-3} kcal mol^{-1} (Figure 5a,b). At a distance of around 1 nm between PTN and PTN_{1-6}, two possible free energy minima were observed (Figure 3b). One of these minima corresponds to a mostly nonhelical configuration, and the other, to a configuration exhibiting around six α-helical residues. The minimum in Figure 5b corresponds to α-helical structure, as shown in Figure 5c. To confirm that there is an interaction between peptides, the free energy surfaces versus the distance between the peptides' centromers and versus the number of hydrogen bonds between them were calculated (Figure 5d,e). These calculations show that, in the minimum, PTNs form around eight hydrogen bonds, whereas PTN/PTN_{1-6} forms around three. These data and the fact that PTN and PTN_{1-6} separate in the equilibrium simulations suggest that peptide aggregation may occur but that the aggregates are more weakly connected than that with PTNs. Figure 5f shows that around three to four hydrogen bonds between peptides in the mixture correspond to six to seven α-helical residues. The structure with increased helical content corresponds to a more amphipathic conformation, which is often correlated with increased biological activity.

The interaction between the peptides and the micelle in terms of the hydrogen bonds was investigated in the equilibrium simulations. Approximately seven hydrogen bonds are formed by the two PTNs, and PTN with PTN_{1-6} forms 9. In the first hydration layer, PTNs coordinate three SO_4^{2-} head groups, whereas PTN/PTN_{1-6} coordinates 5.5. These data suggest a stronger interaction of the peptide mixture with the micelle than that with pure PTN. The replica exchange simulations also showed a more favorable interaction of the peptide mixture with the micelle. Figure 6 presents the free energy surface versus the distance between the peptides' centromers considering the Coulomb and Lennard-Jones contributions (pairwise averaged). Although PTNs are closer to each other than PTN and PTN_{1-6}, the Coulomb contribution of the former pair is in the same range as that

DOI: 10.1021/bi501210e
Biochemistry 2015, 54, 2262−2269

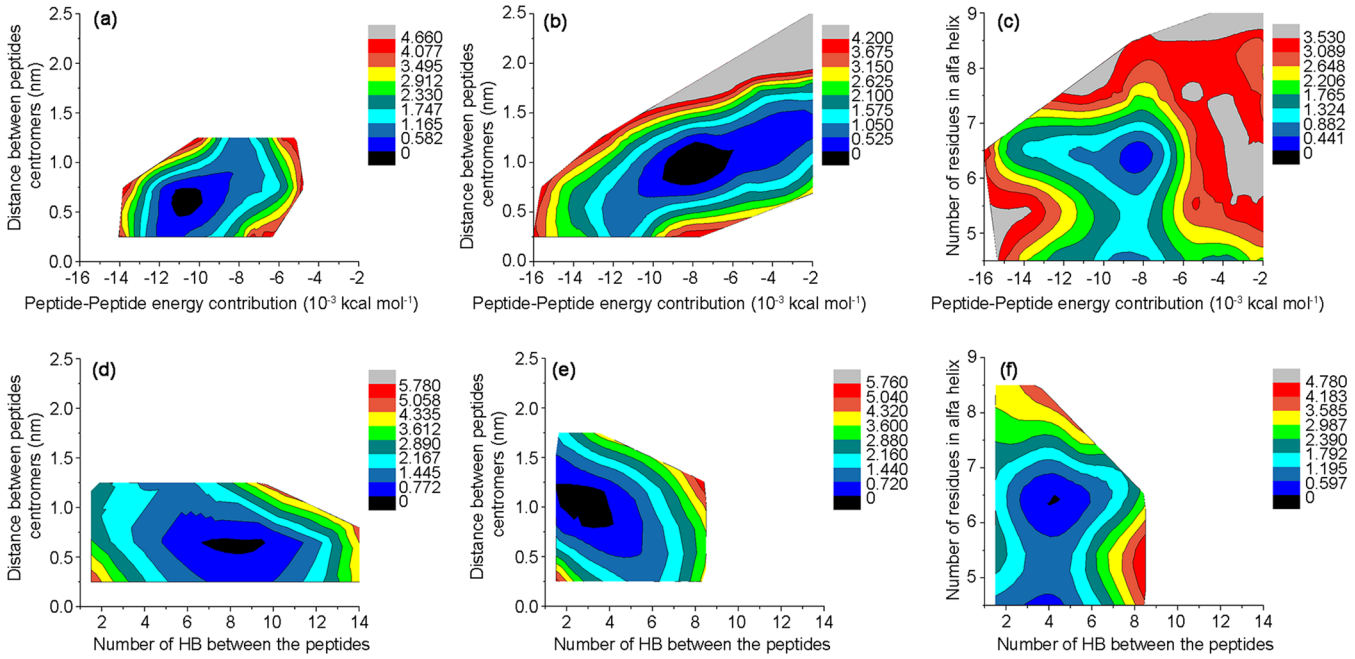

Figure 5. Free energy map (kcal mol^{-1}) for the peptide−peptide interaction. (a−c) Coulomb plus Lennard-Jones energy contributions, pairwise averaged, versus the distance between the peptides' centromers for (a) PTNs and (b) PTN/PTN$_{1-6}$ and (c) versus the number of α-helical residues for the peptide mixture. (d−f) Number of hydrogen bonds between peptides versus the distance between peptides' centromers for (d) PTNs and (e) PTN/PTN$_{1-6}$ and (f) versus the number of α-helical residues for the peptide mixture.

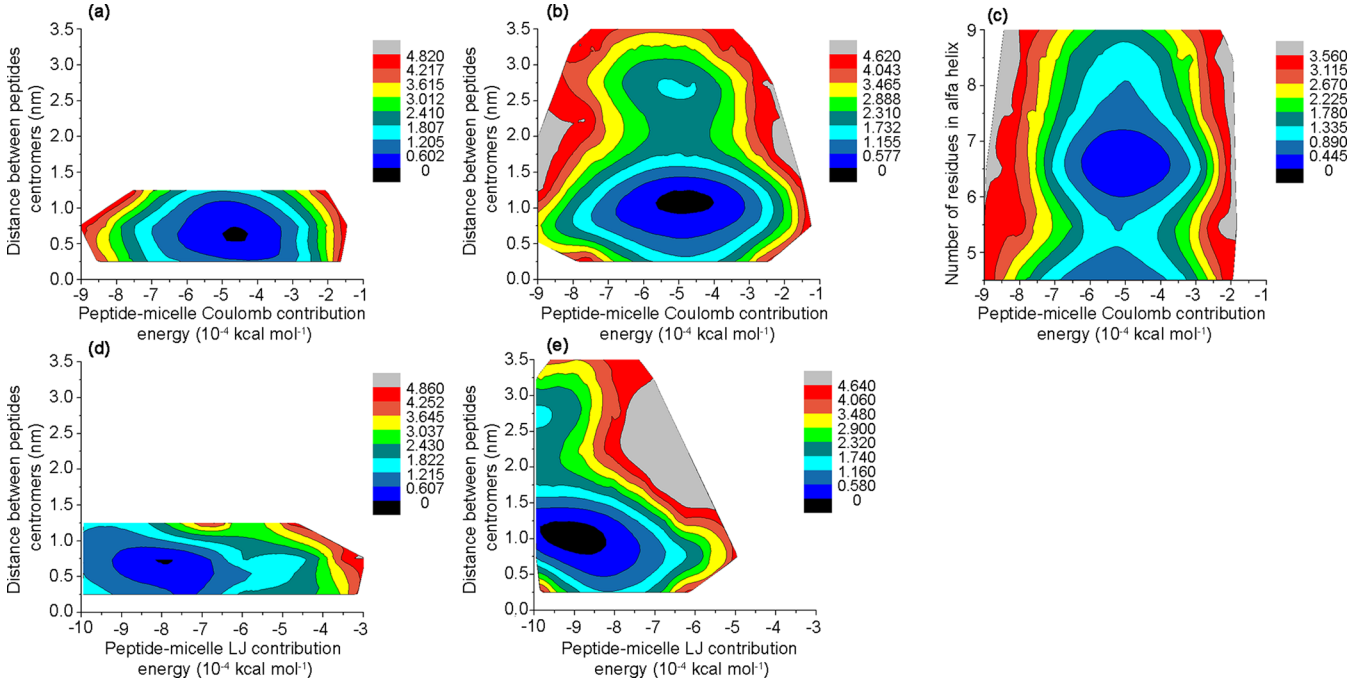

Figure 6. Free energy map (kcal mol^{-1}) of the interaction energy between peptides and the SDS micelle, pairwise averaged. (a−c) Coulomb contribution versus the distance between the peptides' centromers for (a) PTNs and (b) PTN/PTN$_{1-6}$ and (c) versus the number of α-helical residues for the peptide mixture. (d, e) Lennard-Jones contribution versus the distance between the peptides' centromers for (d) PTNs and (e) PTN/PTN$_{1-6}$.

in the latter (Figure 6a,b). The Lennard-Jones contribution for the peptide mixture with the micelle is more favorable than that for the pure PTNs (Figure 6d,e). However, a second minima around the same Coulomb or Lennard-Jones energy level was found with the peptide mixture (Figure 6b,e), which corresponds to a longer distance between the peptides' centromers (approximately at 2.5 nm) and also to six or seven α-helical residues (Figure 6c). The different interaction of PTNs and PTN/PTN$_{1-6}$ with the micelle could be attributed to the existence of this second minimum, in which peptides are separated.

DOI: 10.1021/bi501210e
Biochemistry 2015, 54, 2262−2269

CONCLUSIONS

PTNs exhibit a tendency to aggregate; however, in a system containing PTN_{1-6}, this tendency is reduced. Our results showed that peptides' aggregation, in water and in both systems, is maintained by hydrogen bonds, but when the same systems are placed in the presence of SDS micelles, the number of hydrogen bonds increases between pure PTNs and decreases for the PTN/PTN_{1-6} mixture. The REMD simulations showed that peptides, in the pure or mixed condition, aggregate differently due to the more favorable sum of the Coulomb and Lennard-Jones contributions to the interaction energy of the system with pure PTN. The weaker sum of contributions in the peptide mixture influences the distance between them and the number of α-helical residues. PTN in the PTN/PTN_{1-6} system shows higher helical content and amphipathicity than that of pure PTN. Moreover, there is a favorable interaction of the isolated peptides with the micelle, which does not occur with pure PTNs. Thus, we speculate that a PTN analog with missing residues, as in PTN_{1-6}, decreases the chances of peptide−peptide interactions and enables the longer PTN to more frequently interact with the micelle by generating a more helical and amphipathic structure. These features could be related to the improved antimicrobial activity of PTN, in the micromolar range, caused by the presence of a shorter peptide such as PTN_{1-6}.

ASSOCIATED CONTENT

Supporting Information

Circular dichroism spectra of peptides, secondary structure profile, and potential energy distribution as obtained from molecular dynamics simulations. This material is available free of charge via the Internet at http://pubs.acs.org.

AUTHOR INFORMATION

Corresponding Author

*Tel.: 55-17-32212289. Fax: 55-17-32212356. E-mail: cabrera.marcia@gmail.com.

Funding

This work was supported in part by grants from Fundação de Amparo à Pesquisa do Estado de São Paulo (FAPESP) (2010/11823-0 and 2014/08372-7 to M.P.d.S.C), and BIOprospec-TA/FAPESP program (2006/57122-7). G.B. was Capes fellowship recipient. J.R.R. is a CNPq researcher (307226/2009-3).

Notes

The authors declare no competing financial interest.

ACKNOWLEDGMENTS

The authors acknowledge MSc Tamara R. Valder for implementing the SDS simulation boxes and Prof. Dr. Vitor Barbanti Pereira Leite for providing computational resources. The authors thank Dra. Bibiana Monson de Souza and Prof. Dr. Mario Sergio Palma for preparing and supplying peptides samples and Prof. Dr. João Ruggiero Neto for the use of the circular dichroism spectropolarimeter.

ABBREVIATIONS

MD, molecular dynamics; AMP, antimicrobial peptides; REMD, replica exchange molecular dynamics; SDS, sodium dodecyl sulfate; WHAM, weighted histogram analysis method; LJ, Lennard-Jones; RMSD, root-mean-square deviation

REFERENCES

(1) Xu, X., Li, J., Lu, Q., Yang, H., Zhang, Y., and Lai, R. (2006) Two families of antimicrobial peptides from wasp (*Vespa magnifica*) venom. *Toxicon 47*, 249−253.

(2) De Souza, B. M., Da Silva, A. V., Resende, V. M., Arcuri, H. A., dos Santos Cabrera, M. P., Ruggiero Neto, J., and Palma, M. S. (2009) Characterization of two novel polyfunctional mastoparan peptides from the venom of the social wasp *Polybia paulista*. *Peptides 30*, 1387−1395.

(3) Mendes, M. A., De Souza, B. M., and Palma, M. S. (2005) Structural and biological characterization of three novel mastoparan peptides from the venom of the neotropical social wasp *Protopolybia exigua* (Saussure). *Toxicon 45*, 101−106.

(4) Findlay, B., Zhanel, G. G., and Schweizer, F. (2010) Cationic amphiphiles, a new generation of antimicrobials inspired by the natural amtimicrobial peptide scaffold. *Antimicrob. Agents Chemother. 54*, 4049−4058.

(5) Matsuzaki, K. (2009) Control of cell selectivity of antimicrobial peptides. *Biochim. Biophys. Acta 1788*, 1687−1692.

(6) Hoskin, D. W., and Ramamoorthy, A. (2008) Studies on anticancer activities of antimicrobial peptides. *Biochim. Biophys. Acta 1778*, 357−375.

(7) Nishida, M., Imura, Y., Yamamoto, M., Kobayashi, S., Yano, Y., and Matsuzaki, K. (2007) Interaction of a magainin−PGLa hybrid peptide with membranes: insight into the mechanism of synergism. *Biochemistry 46*, 14284−14290.

(8) Haney, E. F., Hunter, H. N., Matsuzaki, K., and Vogel, H. J. (2009) Solution NMR studies of amphibian antimicrobial peptides: linking structure to function? *Biochim. Biophys. Acta 1788*, 1639−1655.

(9) Matsuzaki, K., Mitani, Y., Akada, K. Y., Murase, O., Yoneyama, S., Zasloff, M., and Miyajima, K. (1998) Mechanism of synergism between antimicrobial peptides magainin 2 and PGLa. *Biochemistry 37*, 15144−15153.

(10) Hara, T., Mitani, Y., Tanaka, K., Uematsu, N., Takakura, A., Tachi, T., Kodama, H., Kondo, M., Mori, H., Otaka, A., Nobutaka, F., and Matsuzaki, K. (2001) Heterodimer formation between the antimicrobial peptides magainin 2 and PGLa in lipid bilayers: a cross-linking study. *Biochemistry 40*, 12395−12399.

(11) Tremouilhac, P., Strandberg, E., Wadhwani, P., and Ulrich, A. S. (2006) Synergistic transmembrane alignment of the antimicrobial heterodimer PGLa/magainin. *J. Biol. Chem. 281*, 32089−32094.

(12) Mor, A., Hani, K., and Nicolas, P. (1994) The vertebrate peptide antibiotics dermaseptins have overlapping structural features but target specific microorganisms. *J. Biol. Chem. 269*, 31635−31641.

(13) Rosenfeld, Y., Barra, D., Simmaco, M., Shai, Y., and Mangoni, M. L. (2006) A synergism between temporins toward Gram-negative bacteria overcomes resistance imposed by the lipopolysaccharide protective layer. *J. Biol. Chem. 281*, 28565−28574.

(14) Mendes, M. A., De Souza, B. M., Marques, M. R., and Palma, M. S. (2004) Structural and biological characterization of two novel peptides from the venom of the neotropical social wasp *Agelaia pallipes pallipes*. *Toxicon 44*, 67−74.

(15) Dohtsu, K., Okumura, K., Hagiwara, K., Palma, M. S., and Nakajima, T. (1993) Isolation and sequence analysis of peptides from the venom of *Protonectarina sylveirae* (Hymenoptera-Vespidae). *Nat. Toxins 1*, 271−276.

(16) Baptista-Saidemberg, N. B., Saidemberg, D. M., De Souza, B. M., Cesar-Tognoli, L. M., Ferreira, V. M., Mendes, M. A., dos Santos Cabrera, M. P., Ruggiero Neto, J., and Palma, M. S. (2010) Protonectin (1−6): a novel chemotactic peptide from the venom of the social wasp *Agelaia pallipes pallipes*. *Toxicon 56*, 880−889.

(17) Fukunishi, H., Watanabe, O., and Takada, S. (2002) On the Hamiltonian replica exchange method for efficient sampling of biomolecular systems: Application to protein structure predicition. *J. Chem. Phys. 16*, 9058−9067.

(18) Periole, X., and Mark, A. E. (2007) Convergence and sampling efficiency in replica exchange simulations of peptide folding in explicit solvent. *J. Chem. Phys. 126*, 014903−1−014903−11.

DOI: 10.1021/bi501210e
Biochemistry 2015, 54, 2262−2269

(19) Rhee, Y. M., and Pande, V. S. (2003) Multiplexed-replica exchange molecular dynamics method for protein folding simulation. *Biophys. J. 84*, 775−786.
(20) Rajendran, V., Purohit, R., and Sethumadhavan, R. (2012) In silico investigation of molecular mechanism of laminopathy caused by a point mutation (R482W) in lamin A/C protein. *Amino Acids 43*, 603−615.
(21) Herce, H. D., Garcia, A. E., Litt, J., Kane, R. S., Martin, P., Enrique, N., Rebolledo, A., and Milesi, V. (2009) Arginine-rich peptides destabilize the plasma membrane, consistent with a pore formation translocation mechanism of cell-penetrating peptides. *Biophys. J. 97*, 1917−1925.
(22) Sengupta, D., Leontiadou, H., Mark, A. E., and Marrink, S. J. (2008) Toroidal pores formed by antimicrobial peptides show significant disorder. *Biochim. Biophys. Acta 1778*, 2308−2317.
(23) Carotenuto, A., Malfi, S., Saviello, M. R., Campiglia, P., Gomez-Monterrey, I., Mangoni, M. L., Gaddi, L. M., Novellino, E., and Grieco, P. (2008) A different molecular mechanism underlying antimicrobial and hemolytic actions of Temporins A and L. *J. Med. Chem. 51*, 2354−2362.
(24) Wang, Q., Hong, G., Johnson, G. R., Pachter, R., and Cheung, M. S. (2010) Biophysical properties of membrane-active peptides based on micelle modeling: a case study of cell-penetrating and antimicrobial peptides. *J. Phys. Chem. B 114*, 13726−13735.
(25) Zagrovic, B., Gattin, Z., Lau, J. K., Huber, M., and van Gunsteren, W. F. (2008) Structure and dynamics of two beta-peptides in solution from molecular dynamics simulations validated against experiment. *Eur. Biophys. J. 37*, 903−912.
(26) Saviello, M. R., Malfi, S., Campiglia, P., Cavalli, A., Grieco, P., Novellino, E., and Carotenuto, A. (2010) New insight into the mechanism of action of the temporin antimicrobial peptides. *Biochemistry 49*, 1477−1485.
(27) Khandelia, H., Langham, A. A., and Kaznessis, Y. N. (2006) Driving engineering of novel antimicrobial peptides from simulations of peptide-micelle interactions. *Biochim. Biophys. Acta 1758*, 1224−1234.
(28) Tian, J., Sethi, A., Anunciado, D., Vu, D. M., and Gnanakaran, S. (2012) Characterization of a disordered protein during micellation: interactions of α-synuclein with sodium dodecyl sulfate. *J. Phys. Chem. B 116*, 4417−4424.
(29) Jalili, S., and Akhavan, M. (2011) Study of the Alzheimer's Aβ40 peptide in SDS micelles using molecular dynamics simulations. *Biophys. Chem. 153*, 179−186.
(30) Gomes-Neto, F., Valente, A. P., and Almeida, F. C. L. (2013) Modeling the interaction of dodecylphosphocholine micelle with the anticoccidial peptide PW2 guided by NMR data. *Molecules 18*, 10056−10080.
(31) Srinivasan, R. *RIBOSOME—Program to build coordinates for peptides from sequence*, Johns Hopkins University, Baltimore, MD, http://folding.chemistry.msstate.edu/~raj/Manuals/ribosome.html.
(32) Valder, T. R. (2010) Interação do Peptídeo MP-I com micela de SDS em Solução Aquosa: Um Estudo por Dinâmica Molecular. Dissertação de Mestrado—Instituto de Biociências, Letras e Ciências Exatas de São José do Rio Preto, Universidade Estadual Paulista Julio de Mesquita Filho, São José do Rio Preto. http://base.repositorio.unesp.br/bitstream/handle/11449/87543/valder_tr_me_sjrp.pdf?sequence=1&isAllowed=y.
(33) Jusufi, A., Hynninen, A. P., and Panagiotopoulos, A. Z. (2008) Implicit solvent models for micellization of ionic surfactants. *J. Phys. Chem. B 112*, 13783−13792.
(34) Zana, R. (2005) *Dynamics of Surfactant Self-Assemblies: Micelles, Microemulsions, Vesicles, and Lyotropic Phases*, Vol. *125*, CRC Press, Boca Raton, FL.
(35) Bruce, C. D., Berkowitz, M. L., Perera, L., and Forbes, M. D. E. (2002) Molecular dynamics simulation of sodium dodecyl sulfate micelle in water: micellar structural characteristics and counterion distribution. *J. Phys. Chem. B 106*, 3788−3793.
(36) Mackerell, D. A., Jr. (1995) Molecular dynamics simulation of a sodium dodecyl sulfate micelle in aqueous solution fluidity of the micelle hydrocarbon interior. *J. Phys. Chem. 99*, 1846−1855.
(37) Rakitin, A. R., and Pack, G. R. (2004) Molecular dynamics simulation of ionic interactions with dodecyl sulfate micelles. *J. Phys. Chem. B 108*, 2712−2716.
(38) Shang, B. Z., Wang, Z., and Larson, R. G. (2008) Molecular dynamics simulation of interaction between a sodium dodecyl sulfate micelle and poly(ethylene oxide) polymer. *J. Phys. Chem. B 112*, 2888−2900.
(39) Berendsen, H. J. C., van der Spoel, D., and van Drunen, R. (1995) GROMACS: a message-passing parallel molecular dynamics implementation. *Comput. Phys. Commun. 91*, 43−56.
(40) Hess, B., Kutzner, C., van Der Spoel, D., and Lindahl, E. (2008) GROMACS 4: algorithms for highly efficient, load-balanced, and scalable molecular simulation. *J. Chem. Theory Comput. 4*, 435−447.
(41) Scott, W. R. P., Hünenberger, P. H., Tironi, I. G., Mark, A. E., Billeter, S. R., Torda, A. E., Huber, T., Krüger, P., and Van Gunsteren, W. F. (1999) The GROMOS biomolecular simulation program packege. *J. Phys. Chem. A 103*, 3596−3607.
(42) van Gunsteren, W. F., Billeter, S. R., Eising, A. A., Hunenberger, P. H., Kruger, P., Mark, A. E., Scott, W. R. P., and Tironi, I. G. (1996) *Biomolecular Simulation: The GROMOS96 Manual and User Guide*, pp 1−1042, Vdf Hochschulverlag AG an der ETH Zurich, Zurich, Switzerland.
(43) Schuler, L. D., Daura, X., and van Gunsteren, W. F. (2001) An improved GROMOS96 force field for aliphatic hydrocarbons in the condensed phase. *J. Comput. Chem. 22*, 1205−1218.
(44) Soares, T. A., Daura, X., Oostenbrink, C., Smith, L. J., and van Gunsteren, W. F. (2004) Validation of the GROMOS force-field parameter set 45A3 against nuclear magnetic resonance data of hen egg lysozyme. *J. Biomol. NMR 30*, 407−422.
(45) Sammalkorpi, M., Karttunen, M., and Haataja, M. (2007) Structural properties of ionic detergent aggregates: a large-scale molecular dynamics study of sodium dodecyl sulfate. *J. Phys. Chem. B 111*, 11722−11733.
(46) Darden, T., York, D., and Pedersen, L. (1993) Particle mesh Ewald: An $N\cdot\log(N)$ method for Ewald sums in large systems. *J. Chem. Phys. 98*, 10089−10092.
(47) Essmann, U., Perera, L., Berkowitz, M. L., Darden, T., Lee, H., and Pedersen, L. G. (1995) A smooth particle mesh Ewald potential. *J. Chem. Phys. 103*, 8577−8592.
(48) Hess, B., Bekker, H., Berendsen, H. J. C., and Fraaije, J. G. E. (1997) LINCS: A linear constraint solver for molecular simulations. *J. Comput. Chem. 18*, 1463−1472.
(49) Miyamoto, S., and Kollman, P. A. (1992) SETTLE: an analytical version of the SHAKE and RATTLE algorithm for rigid water models. *J. Comput. Chem. 13*, 952−962.
(50) Berendsen, H. J. C., Postma, J. P. M., van Gunsteren, W. F., and Hermans, J. (1981) Interaction models for water in relation to protein hydration, in *Intermolecular Forces* (Pullman, B, Ed.) pp 331−342, Reidel Publishing Co, Dordrecht, The Netherlands.
(51) Kumar, S., Bouzida, D., Swendsen, R. H., Kollman, P. A., and Rosenberg, J. M. (1992) The weighted histogram analysis method for free-energy calculations on biomolecules. I. The method. *J. Comput. Chem. 13*, 1011−1021.
(52) Kumar, S., Bouzida, D., Swendsen, R. H., Kollman, P. A., and Rosenberg, J. M. (1995) Multidimensional free-energy calculations using the weighted histogram analysis method. *J. Comput. Chem. 16*, 1339−1350.

DOI: 10.1021/bi501210e
Biochemistry 2015, 54, 2262−2269